

AD-A169 398

RELAXATION PROPERTIES OF SOME SEGMENTED
POLYURETHANE-CACO₃ COMPOSITES R. D. (U) MASSACHUSETTS
UNIV AMHERST DEPT OF POLYMER SCIENCE AND ENGINE.

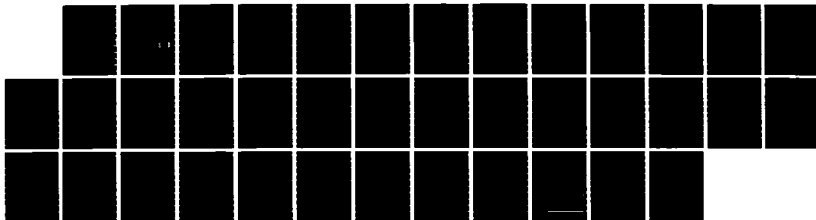
1/1

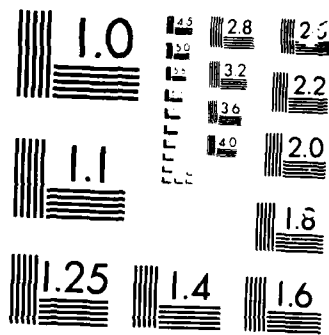
UNCLASSIFIED

J C CHIEN ET AL. 08 MAY 86 TR-14

F/G 11/4

NL





MICROSCOPE

100X

12

AD-A169 398

OFFICE OF NAVAL RESEARCH

Task # 659-795

Contract # N00014-85-K-0880

Technical Report No. 14

RELAXATION PROPERTIES OF SOME SEGMENTED POLYURETHANE-CaCO₃
COMPOSITES. A DIELECTRIC STUDY

James C.W. Chien, Principal Investigator
University of Massachusetts
Department of Polymer Science and Engineering
Amherst, MA 01003
Telephone: (413) 545-2727

May 8, 1986

DTIC
SELECTED
JUL 03 1986
S D

Reproduction in whole or in part is permitted for any
purpose by the United States Government

*This document has been approved for public
release and sale; its distribution is unlimited.*

DTIC FILE COPY

86 7 3 012

Relaxation Properties of Some Segmented Polyurethane-CaCO₃
Composites. A Dielectric Study.

György Bánhegyi*, Man-Khyun Rho, James C.W. Chien, Frank E. Karasz

Polymer Science and Engineering Department
University of Massachusetts
Amherst, MA 01003

| | | |
|--------------------|----------------------|-------------------------------------|
| Accession For | | |
| NTIS | CRA&I | <input checked="" type="checkbox"/> |
| DTIC | TAB | <input type="checkbox"/> |
| Unannounced | | <input type="checkbox"/> |
| Justification | | |
| By | | |
| Distribution/ | | |
| Availability Codes | | |
| Dist | Avail and/or Special | |
| A-1 | | |

*To whom all correspondence should be addressed.
Present address: Research Institute for Plastics,
H-1950
Budapest, HUNGARY

Abstract

Dielectric relaxation in three segmented polyurethane - CaCO_3 composites was investigated between -70°C and $+150^\circ\text{C}$ in the 300 Hz to 100 kHz frequency range. Two of the polymers contained a polyacetal-polyether soft segment, while the soft component of the third polymer was polypropylene oxide. The hard segments consisted of 4,4'-diphenyl methane diisocyanate in two cases and toluene-2,4-diisocyanate in the third case.

In parallel studies two calorimetric relaxations, designated α and α' , were observed for each sample and were determined to be glass transitions of the soft and hard segments, respectively. In general, the transition temperatures decrease with increasing filler content. High frequency, low temperature permittivities increase while low frequency, high temperature AC conductivities generally decrease with increasing filler content. The shift in the transition temperatures can be explained using the adsorption theory of filler-polymer interactions and the densities of the samples. The interfacial polarization mechanism becomes important only above the α' transition temperature and below 1 kHz.

Introduction

Segmented polyurethanes are useful and versatile materials whose properties can be varied within a wide range depending on the chemical structures and the molecular weights of the soft and hard segments. Typical morphological and physical properties of the segmented polyurethanes have been summarized.(1-4)

In the present work the physical properties of some specially synthesized filled polyurethanes exhibiting good thermal stability were studied with the purpose of understanding the polymer-filler interaction and the effect of filler content on the dielectric relaxation; detailed results for the dynamic mechanical and scanning calorimetric studies will be published elsewhere.(5)

Experimental

Three different classes of segmented polyurethanes with 0, 25, 40 and 60 volume % filler contents were synthesized and studied.

The hard segment of the polymers designated A and B (Figure 1) contained 4,4'-diphenyl methane diisocyanate (MDI; Mobay Chemicals). The chain extender was N,N'-bis(2-hydroxyethyl)-isophthalamide (BI) synthesized from the isophthalate ester by aminolysis using 2-aminoethanol (Aldrich Chemical Co.). The soft segment of polymer A was a polyacetal (PAC) synthesized from valeraldehyde and diethylene glycol (Aldrich Chemical Co.) and having a molecular weight of about 1800. The soft segment of polymer B was polypropylene oxide (PPO; Polysciences) with a molecular weight of about 2000. In the case of the polymer designated C the soft segment was again the valeraldehyde-diethyleneglycol polyacetal (PAC); the hard segment, however, contained toluene-2,4-diisocyanate (TDI; Aldrich

Chemical Co.).

The synthesis was performed in two steps: first the diisocyanate was reacted with the soft segment (polyol) in a molar ratio of 2:1 and then the chain extender (1 mole) was added. Further details of the synthesis will be published elsewhere.(5)

Fig. 1 shows the chemical structures of polymers A, B and C. The calcium carbonate filler used (Gamma Sparse® 6451; Georgia Marble Co.) had an average particle size of 5.5µm.

Samples were compression molded from the powdered polyurethanes at 110°C and 130 atm, for 20 min. The code used below indicates the polymer type, A, B or C, and the filler content; for example B25 represents 25 volume % filler in the polymer matrix of type B.

Measurements

The densities of the samples were determined gravimetrically.

Dielectric measurements were performed using a General Radio 1620 Capacitance Bridge at 300 Hz, 1 kHz, 3 kHz, 10 kHz, 50 kHz and 100 kHz. The samples were placed in a three terminal Balsbaugh TTRC-64 cell with an active electrode diameter of 5.5 cm. The sample thickness was around 0.5 mm. The dielectric dispersion (ϵ') and loss (ϵ'') curves were calculated from the measured capacitance (C) and dissipation factor ($\tan \delta$) by the following standard formulae:

$$\epsilon' = \frac{C}{C_0} \cdot \frac{1}{(1 + \tan^2 \delta)} \quad (1)$$

$$\epsilon'' = \frac{C}{C_0} \cdot \frac{\tan \delta}{(1 + \tan^2 \delta)} \quad (2)$$

where C_0 is the capacitance of the empty sample holder. The temperature dependence of C_0 has been taken into account in this analysis. Measurements were performed between -70°C and $+150^\circ\text{C}$. Below room temperature, the temperature of the sample holder was regulated by flushing the cell with cooled, prepurified N_2 gas; the temperature was changed by varying the flow rate. Above room temperature an electric heater was used with a Versa-Therm (Model 2156) temperature controller. A flow of dried nitrogen was maintained in the whole temperature range to avoid condensation. The temperature was changed stepwise in about $5\text{-}10^\circ\text{C}$ steps; 10 min. was allowed for equilibration.

Because of difficulties in handling the unfilled polymer C, measurements on this sample were made using a teflon sandwich.

Results

Dielectric dispersion (ϵ') and loss (ϵ'') curves of the unfilled polymers measured at 100 kHz and plotted versus temperature are shown in Fig. 2. To demonstrate the presence of the two transitions, denoted here as α and α' , the highest frequency was selected; at lower frequencies the high temperature loss peaks (α') are obscured by the presence of ohmic conductivity. Dispersion and loss curves of polymer A at four different frequencies are presented in Fig. 3. Transition α' appears only as a shoulder at 10 kHz and becomes totally observed by the conductivity tail at lower frequencies.

Polymer B0 is slightly more polar than A0. Sample C0 could not be compared directly to the other two, as its dispersion and loss curves are altered by the presence of the teflon foils. Comparison of other samples containing equal amounts of filler (see below) shows that C is the most polar material.

Figures 4, 5 and 6 show the 100 kHz dispersion and loss curves for the A, B and C series, respectively. Losses are normalized as ϵ''/v_1 where v_1 is the volume fraction of the polymer; loss maxima are proportional to the relaxation strength of the polymer which is, in turn, proportional to the number of dipoles per unit volume.⁽⁶⁾ Thus if it is assumed that the filler has no effect other than diluting the polymer, dividing by v_1 should eliminate this effect. (In fact the effect of the filler is more complicated as indicated in the Discussion.)

Figures 7, 8 and 9 show the difference between the low frequency (300 Hz) and high frequency (100 kHz) permittivities as a function of temperature. This difference should be equal to zero far from the relaxation regions and should show a maximum in the transition temperature range. Therefore, the shapes of these curves should be similar to those of the losses. The advantage of this representation is the elimination of ohmic conductivity effects which contribute only to the imaginary part of the dielectric constant. The sharp increase of the permittivity difference at higher temperatures for the samples with higher filler contents is probably due to the appearance of an interfacial loss mechanism.

Arrhenius plots for the α -transitions of the A and B series are shown in Figure 10. The activation energies of the α' transitions could not be calculated because of the strong effect of conductivity at lower frequencies. In principle, the true dielectric loss, ϵ''_D , can be calculated from the total loss, ϵ''_{tot} , by subtracting the ohmic conductivity:⁽⁶⁾

$$\epsilon''_D = \epsilon''_{tot} - \frac{\sigma_0}{2\pi\nu\epsilon_0} \quad (3)$$

where σ_0 is the ohmic (DC) conductivity, ϵ_0 is the vacuum permittivity

(8.854×10^{-2} pF/cm), and ν is the frequency at which the measurements were made. This procedure can be carried out, however, only in a temperature range where ϵ''_0 is small, i.e. where the total loss is entirely due to the ohmic conductivity. In this case, ϵ_0 can be determined in the temperature range of the transition by extrapolation. In this instance, however, this procedure cannot be used because the AC conductivity is frequency dependent throughout the temperature range studied. Figure 11 shows the Arrhenius plot for the AC conductivities measured at 300 Hz.

In the case of the C-series polymers, transition α appears as a shoulder on the high temperature loss peak only, thus the peak shift could not be determined accurately. Table 1 summarizes the 100 kHz peak temperatures and the activation energies, whenever available.

Table 2 shows the measured and calculated densities of the composites. The calculations were performed assuming volume additivity and using the densities of the pure polymeric components and 2.71 g/cm^3 for CaCO_3 .

Discussion

Figures 2-9 clearly show the presence of two transitions in both the unfilled polymers and in the composites. One of the transitions, labelled α , occurs close to 0°C , the other, labelled α' , occurs between 80°C and 120°C . There is some evidence that a transition exists below -80°C as well, but this was not studied. Based on earlier dielectric studies on segmented polyurethanes,⁽⁷⁻¹¹⁾ the α transition can be assigned to the glass transition of the soft segments; this is also supported by dynamic mechanical spectra.⁽⁵⁾ The interfacial dielectric loss mechanism due to microphase separation, which is

very important in some segmented polyurethanes,⁽⁷⁻⁹⁾ seems to be insignificant in the A0, B0 and C0 samples, at least in the frequency and temperature ranges studied. There is some indication that dielectric loss due to microphase separation occurs above 100°C and below 1 kHz in the filled samples.

Interpretation of the high temperature transition, α' , is not so obvious. The presence of the α' transition in segmented polyurethanes has been demonstrated previously by scanning calorimetry, and by thermomechanical and dynamic mechanical measurements.⁽¹²⁻¹⁶⁾ These studies revealed that there were basically two transitions above the soft segment glass transition (α), one around 70-80°C (α') and another at 150-180°C (α''). It was demonstrated⁽¹³⁾ that the first transition could be shifted to a higher temperature by annealing. Based on a combined thermal, IR and morphological study,⁽¹⁴⁾ both transitions were attributed to morphological (short-range order) effects involving the hard segments.

Interactions between hard and soft segments are obvious (see Table 1 and Figure 1); for example, the hard segments of series A and B or the soft segments of A and C are identical while the transition temperatures are different.

In studying the transition temperatures as a function of filler content (Table 1) the following conclusions can be drawn concerning the polymer-filler interaction. In series A, (Figures 4 and 7) addition of 25 volume % filler produces small increases in the transition temperatures and the activation energy of the soft segment transition (α). The experimental density is higher than the calculated density (Table 2) which could be due to a strong adhesive bonding between the polymer and the CaCO_3 filler.⁽¹⁷⁾ In contrast addition of 40 volume % CaCO_3 minimally affects the transition temperatures. The loss maxima decrease

and the experimental density becomes lower than the calculated value. At the highest filler content, transition temperatures and loss maxima decrease still further. The decrease of the transition temperatures can be explained by the additional free volume formed around aggregated filler particles.⁽¹⁷⁾ Despite this "loosening" of the structure the activation energy for the soft segment transition does not decrease significantly.

It is worth mentioning that the relative height of the α' -loss maxima as compared to the α -loss maxima generally decreases with increasing filler content. The decrease in the loss maxima can be due to the decrease either in the effective dipole moment of the relaxing units or in the number of reorientable dipoles. The latter seems more probable for, if it is assumed that bonding between the polymer and the filler occurs predominantly through the more polar hard segment, the amount of "immobilized", non-orientable, hard segments is expected to increase with increasing filler content.

In series B, (Figures 5 and 8) α and α' transition temperatures decrease with increasing filler content. The intensity of the transition α remains almost unchanged, while that of the hard segment (α') decreases. As for series A the activation energy of the soft segment transition (α) increases at first and then decreases with increasing filler content.

Composites of series C (Figures 6 and 9) behave somewhat differently. In this case the intensity ratio between the low- and high-temperature transitions is reversed due to the higher dipole moment of the TDI unit (hard segment). It is interesting, however, that the intensity of the lower temperature transition is lower than in the A series despite the fact that the soft segments are identical. This again demonstrates the coupling between hard and soft segments.

Addition of 25 volume % filler sharply increases the transition temperatures, especially that of the hard segment ($T_{\alpha 1}$). Further addition of CaCO_3 decreases T_{α} back to the original value. $T_{\alpha 1}$, however, remains practically constant.

Peak temperature shifts mainly parallel the mechanical data but the strong broadening of soft segment transitions observed in mechanical spectra⁽⁵⁾ is not apparent in the dielectric spectra.

The last topic to be discussed concerns the absolute values of the permittivities and the Maxwell-Wagner polarization mechanism in the composites. The permittivities of particulate composites can be calculated from various mixture formulae⁽¹⁸⁾ involving the component permittivities, volume fractions and the shapes of the filler particles.

Two of these formulae will be applied here, the so-called Wagner and Bruggeman formulae.⁽¹⁸⁾ The first describes the composite permittivity ($\bar{\epsilon}$) at low filler concentrations ($v_2 < 0.2$):

$$\bar{\epsilon} = \epsilon_1 \frac{2\epsilon_1 + \epsilon_2 + 2v_2(\epsilon_2 - \epsilon_1)}{2\epsilon_1 + \epsilon_2 - v_2(\epsilon_2 - \epsilon_1)} \quad (4)$$

and the second describes the composite permittivity over the entire concentration range:

$$\left(\frac{\bar{\epsilon} - \epsilon_2}{\epsilon_1 - \epsilon_2} \right)^3 \left(\frac{\epsilon_1}{\bar{\epsilon}} \right) = (1 - v_2)^3 \quad (5)$$

In both cases it is assumed that the filler particles are spherical. At low filler concentrations the two equations give identical results. Figure 12 shows the composite permittivity as a function of the matrix permittivity (ϵ_1).

assuming $\epsilon_2 = 8.0$ for CaCO_3 . (19)

The validity of these formulae could be checked if the high frequency limiting permittivities (ϵ_∞) of the polymers and composites were known. This quantity can be calculated either from the infrared refractive index or from cryogenic high frequency permittivities. In the present study the lowest temperature used was -80°C , so the ϵ_∞ limit was not reached; nevertheless the lowest temperature 100 kHz ϵ' values shown in Figs. 4-6 can be compared to the $\bar{\epsilon}$ values plotted in Fig. 12. Series B and C behave as expected, i.e., the low temperature, high frequency ϵ' values increase with increasing filler content. In the case of series A, ϵ' values of the composites are generally higher than those of the unfilled polymer, but instead of a monotonic increase ϵ' displays a maximum in the case of the A25 sample.

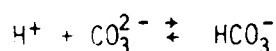
If one or both components of the composite exhibit dielectric relaxation but the ohmic conductivities are insignificant, eqs. (4) and (5) can be used to calculate the frequency dependent composite-permittivity, but instead of ϵ_1 and ϵ_2 , the frequency dependent ϵ_1' and ϵ_2' functions must be substituted. (6,20) The ratio of composite and polymer loss intensities can be given by the following formula if ϵ_2 is constant:

$$\frac{\bar{\epsilon}''(\text{max})}{\epsilon_1''(\text{max})} = \frac{\bar{\epsilon}(\epsilon_1^S) - \bar{\epsilon}(\epsilon_1^\infty)}{\epsilon_1^S - \epsilon_1^\infty} \quad (6)$$

where $\epsilon_1''(\text{max})$ is the loss maximum in the pure polymer, $\bar{\epsilon}''(\text{max})$ is that in the composite, ϵ_1^∞ and ϵ_1^S are the permittivities of the polymers below and above the transition temperature, respectively; $\bar{\epsilon}(\epsilon_1^\infty)$ and $\bar{\epsilon}(\epsilon_1^S)$ are the corresponding composite permittivities. Figure 13 shows the calculated $\bar{\epsilon}''(\text{max})/\epsilon_1''(\text{max})$ values for

a system with $\epsilon_2 = 8.0$; ϵ_1^∞ , ϵ_1^S and v_2 are varied. It can be seen that the theoretical ratios approximate $v_1 = 1 - v_2$ (the expected ratio, if the filler has no other effect than diluting the polymer dipoles) only if $\epsilon_1^S - \epsilon_1^\infty$ is high and ϵ_1^∞ is relatively close to ϵ_2 . Taking this result into account, even constant $\bar{\epsilon}''/v_1$ values (see e.g. Figure 5 in the α transition region) correspond to reduced polymer relaxation strengths which could be an indirect indication of the immobilizing effect of the filler mentioned earlier.

Another interesting feature of the system is that the low frequency (300 Hz) AC conductivity generally decreases with increasing filler content (Fig. 11). The conductivity of calcite is anisotropic and frequency dependent.⁽¹⁹⁾ At room temperature the average value is around $10^{-10} \Omega^{-1} \text{ cm}^{-1}$, which is comparable to that of the pure polymers. Theoretically the composite conductivities can be calculated from eqs. (4) and (5) replacing the permittivities by ohmic conductivities. Systematic decrease of the conductivities with increasing filler loading shows, however, that other factors have to be taken into account. Polyurethanes also contain amide bonds so it is reasonable to assume that the relatively high conductivity ($10^{-9} - 10^{-11} \Omega^{-1} \text{ cm}^{-1}$) is due to proton migration along the H-bond system as in the case of polyamides.⁽²¹⁾ If this is the case, carbonate fillers can effectively retard the mobility of proton by the following reaction:



The conductivity of protons is influenced by the molecular motion of the amide groups. According to a simplified theoretical model of ionic hopping conductivity⁽²²⁾ the AC conductivity should increase with increasing frequency.

This tendency perhaps contributes to the fact that the loss maxima in Figures 4-6 often appear at somewhat higher temperatures than the inflection points of the dispersion curves.

A mixture of two materials with different conductivities and permittivities always exhibits an additional dielectric polarization mechanism, the so called interfacial or Maxwell-Wagner relaxation.⁽¹⁸⁾ The segmented polyurethanes are heterogeneous systems themselves and the presence of an interfacial mechanism can cause permittivities as high as ten at audio- or twenty at subaudio frequencies.^(7,8) In the present case the Maxwell-Wagner effect is not important in the unfilled polymers in the frequency and temperature ranges studied.

The static permittivities $\bar{\epsilon}_s$ and the interfacial relaxation times τ of two component composites containing spherical filler particles can be calculated as:⁽¹⁸⁾

$$\bar{\epsilon}_s = \epsilon_1 \frac{2\sigma_1 + \sigma_2 + 2v_2(\sigma_2 - \sigma_1)}{2\sigma_1 + \sigma_2 - v_2(\sigma_2 - \sigma_1)} \quad (7)$$

$$+ 3v_2\sigma_1 \frac{(2\epsilon_1 + \epsilon_2)(\sigma_2 - \sigma_1) - (2\sigma_1 + \sigma_2)(\epsilon_2 - \epsilon_1)}{[2\sigma_1 + \sigma_2 - v_2(\sigma_2 - \sigma_1)]^2}$$

$$\tau = \epsilon_0 \frac{2\epsilon_1 + \epsilon_2 - v_2(\epsilon_2 - \epsilon_1)}{2\sigma_1 + \sigma_2 - v_2(\sigma_2 - \sigma_1)} \quad (8)$$

These formulae can be derived from the complex analogue of eq. (4). Static permittivities can be calculated from the complex form of eq. (5) (the so-called Hanai formula) as well but in this case there is no explicit expression for the relaxation time, so eqs. (7) and (8) will be used to estimate the interfacial

polarization characteristics of the filled composites.

Table 3 lists the high- and low-frequency limiting permittivities, relaxation times and the frequency maxima for the interfacial relaxation of a model composite containing $v_2 = 0.40$ (40 vol % filler). Component parameters ($\epsilon_1, \epsilon_2, \sigma_1, \sigma_2$) are reasonable estimates. Three permittivity levels are distinguished (2.5, 5.0 and 7.0), one below the α transition, the second between T_{α} and $T_{\alpha'}$, and finally a third above the α' transition. Two values of matrix conductivity are chosen because the conductivities of the pure components differ from each other; σ_2 values are based on literature values(20); $\bar{\epsilon}_{\infty}$ of the composites have been calculated using eq. (4), $\bar{\epsilon}_s$ and $\bar{\tau}$ using eqs. (7) and (8), respectively, ν by the following formula:

$$\nu_{\max} = 1/(2\pi\bar{\tau}) \quad (9)$$

The results show that the difference between the high and low frequency limiting permittivities is small because the difference in component conductivities is low. Relaxation times are relatively high; the Maxwell-Wagner effect is expected only at lower frequencies (below 300 Hz). These calculations are in accordance with the observed behavior: the Maxwell-Wagner effect is manifested only at the highest temperatures where the conductivity difference between the components is large enough to produce a significant difference between $\bar{\epsilon}_s$ and $\bar{\epsilon}_{\infty}$.

Conclusion

The dielectric relaxation study of CaCO_3 filled polyurethane composites has shown that:

- there are two main transition regions in the -70 to +150°C temperature range both in the unfilled polymers and in the composites
- the amount of the filler influences both the position and height of the loss maxima corresponding to these transitions
- the transition temperatures generally first increase and then decrease with increasing filler content
- with the exception of series A, the low temperature, high frequency permittivities increase, while low frequency, high temperature AC conductivities decrease with increasing filler content
- in accordance with model calculations, the Maxwell-Wagner effect is evident only at high temperatures and low frequencies.

Acknowledgements

This work was supported in part by AFOSR Grant No. 84-0100. One of us (G.B.) wants to express his thanks to Dr. Peter Hedvig for reading the manuscript and for his advice.

References

1. R. Bonart: *Angew. Makromol. Chem.*, 58-59, 259 (1977).
2. Yu.Yu. Kercha: *Physical Chemistry of Polyurethanes (in Russian)*, Naukovka Dumka, Kiev (1979).
3. P.E. Gibson, M.A. Vallance, S.L. Cooper: *Dev. Block Copolym.*, 1, 217 (1982).
4. C. Hephurn: *Polyurethane Elastomers*, Elsevier, Amsterdam (1982).
5. M.K. Rho, J.C.W. Chien, to be submitted.
6. P. Hedvig: *Dielectric Spectroscopy of Polymers*, A. Hilger, Bristol (1977).
7. A.M. North, J.C. Reid, J.B. Shortall: *Eur. Polym. J.*, 5, 565 (1969).
8. A.M. North, J.C. Reid: *Polym. J.*, 8, 1129 (1972).
9. S.B. Dev, A.M. North, J.C. Reid in: *Dielectric Properties of Polymers*, Ed. F.E. Karasz, Plenum, New York (1972), p.217.
10. C. Delides, R.A. Pethrick: *Eur. Polym. J.*, 17, 675 (1981).
11. M.A. Vallance, A.S. Yeung, S.L. Cooper: *Colloid and Polym. Sci.*, 261, 541 (1983).
12. G.W. Miller, J.H. Saunders: *J. Polym. Sci.*, A1, 8, 1923 (1970).
13. R.W. Seymour, S.L. Cooper: *J. Polym. Sci.*, B9, 689 (1971).
14. R.W. Seymour, S.L. Cooper: *Macromolecules*, 6, 48 (1973).
15. H.N. Ng, A.E. Allegrazza, R.W. Seymour, S.L. Cooper: *Polymer*, 14, 255 (1973).
16. Z. Petrovic, J. Budinski-Simendic: Submitted for publication to *Rubber Chem. Technol.*

References (continued)

17. Yu.S. Lipatov: Physical Chemistry of Filler Polymers (in Russian) Khimiya, Moscow (1977).
18. L.K.H. van Beek: Prog. Diel., 7, 69 (1967).
19. K.S. Rao, K.V. Rao: Z. Phys., 216, 300 (1968).
20. G. Bánhegyi, P. Hedvig: Polym. Bull., 8, 287 (1982).
21. D.A. Seanor: J. Polym. Sci. A2, 6, 463 (1968).
22. H.A. Pohl: J. Polym. Sci. C, 17, 13 (1967).

Table 1

100 kHz transition temperatures ($^{\circ}\text{C}$) and
activation energies ($\text{E}/\text{kJ}/\text{mole}$) of the polyurethane composites.

| Sample | T_{α} | $E_{\text{Act}}(\alpha)$ | T_{α}' |
|--------|--------------|--------------------------|---------------|
| A0 | 16 | 137 | 90 |
| A25 | 20 | 160 | 114 |
| A40 | 18 | 146 | 120 |
| A60 | 14 | 152 | 105 |
| B0 | 20 | 139 | 115 |
| B25 | 16 | 150 | 100 |
| B40 | 15 | 139 | 105 |
| B60 | 10 | 120 | 105 |
| C0 | 5 | | 58 |
| C25 | 15 | | 91 |
| C40 | -3 | | 79 |
| C60 | 0 | | 85 |

Table 2

Measured and calculated densities of the composites.

| Polymer Type | Density (g/cm ³) | | | | |
|--------------|------------------------------|--------|--------|--------|--------|
| | 0 | 25 | 40 | 60 | |
| A | exp. | 1.0996 | 1.5405 | 1.6021 | 1.9928 |
| | calc. | - | 1.5022 | 1.7438 | 2.0658 |
| B | exp. | 1.0632 | 1.4756 | 1.7189 | 1.9634 |
| | calc. | - | 1.4749 | 1.7219 | 2.0513 |
| C | exp. | 1.1073 | 1.4789 | 1.7386 | 2.0004 |
| | calc. | - | 1.5080 | 1.7484 | 2.0689 |

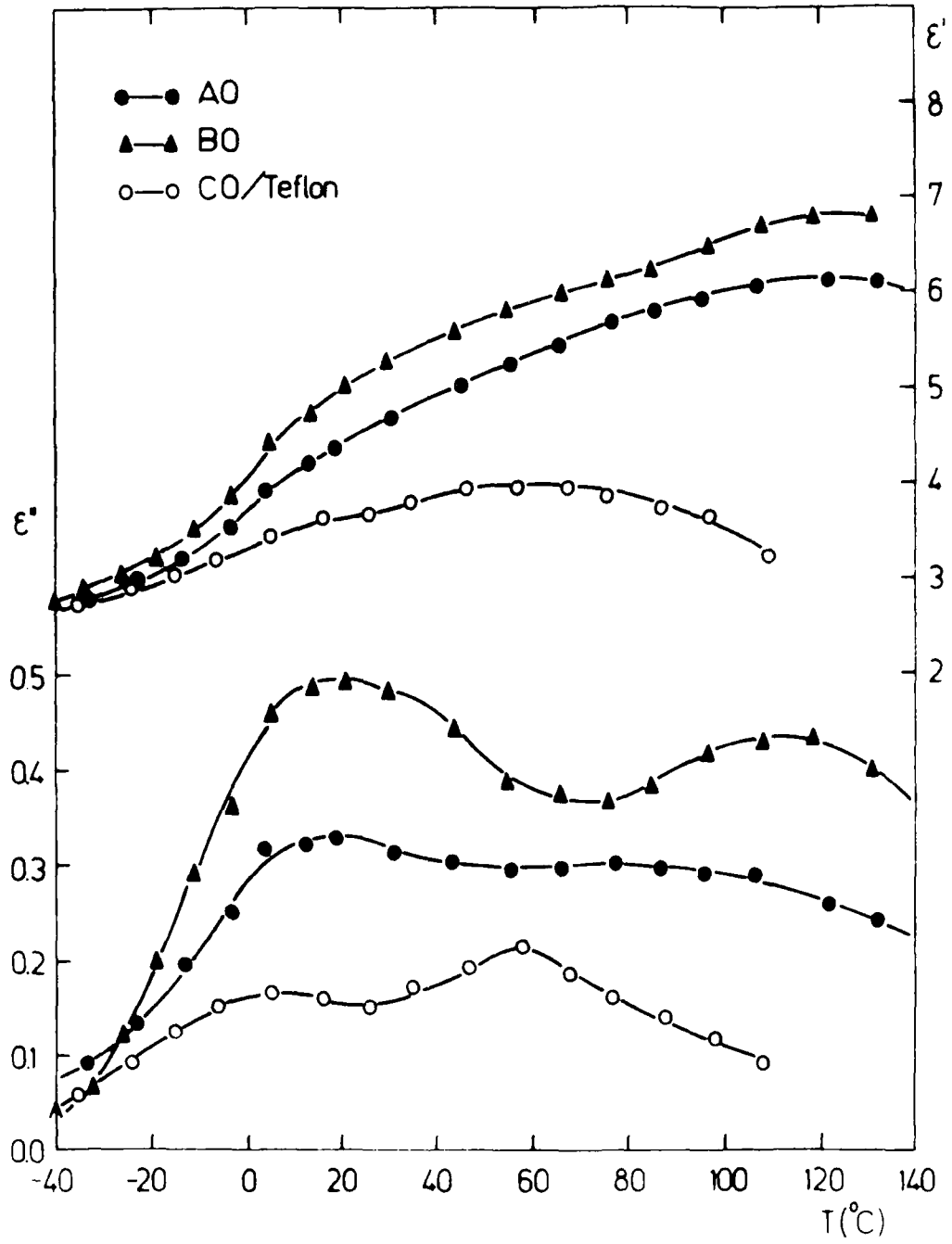
Table 3

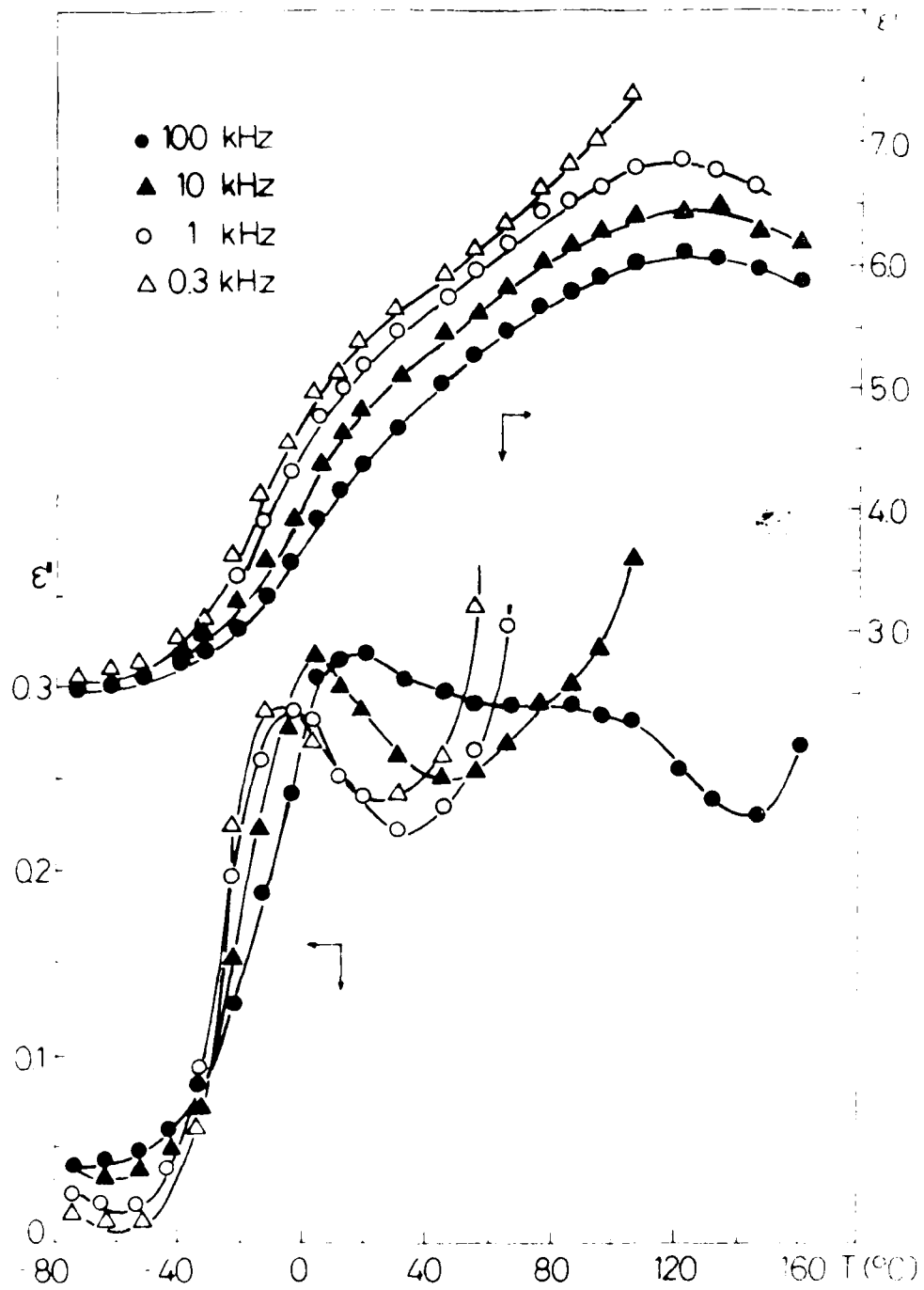
High ($\bar{\epsilon}_\infty$) and low frequency ($\bar{\epsilon}_s$) limiting permittivities. Maxwell-Wagner relaxation time (τ) and maximum frequency (ν_{\max}) for a model composite containing 40 vol% filler as a function of the component properties. Units of conductivity are $\Omega^{-1} \text{ cm}^{-1}$.

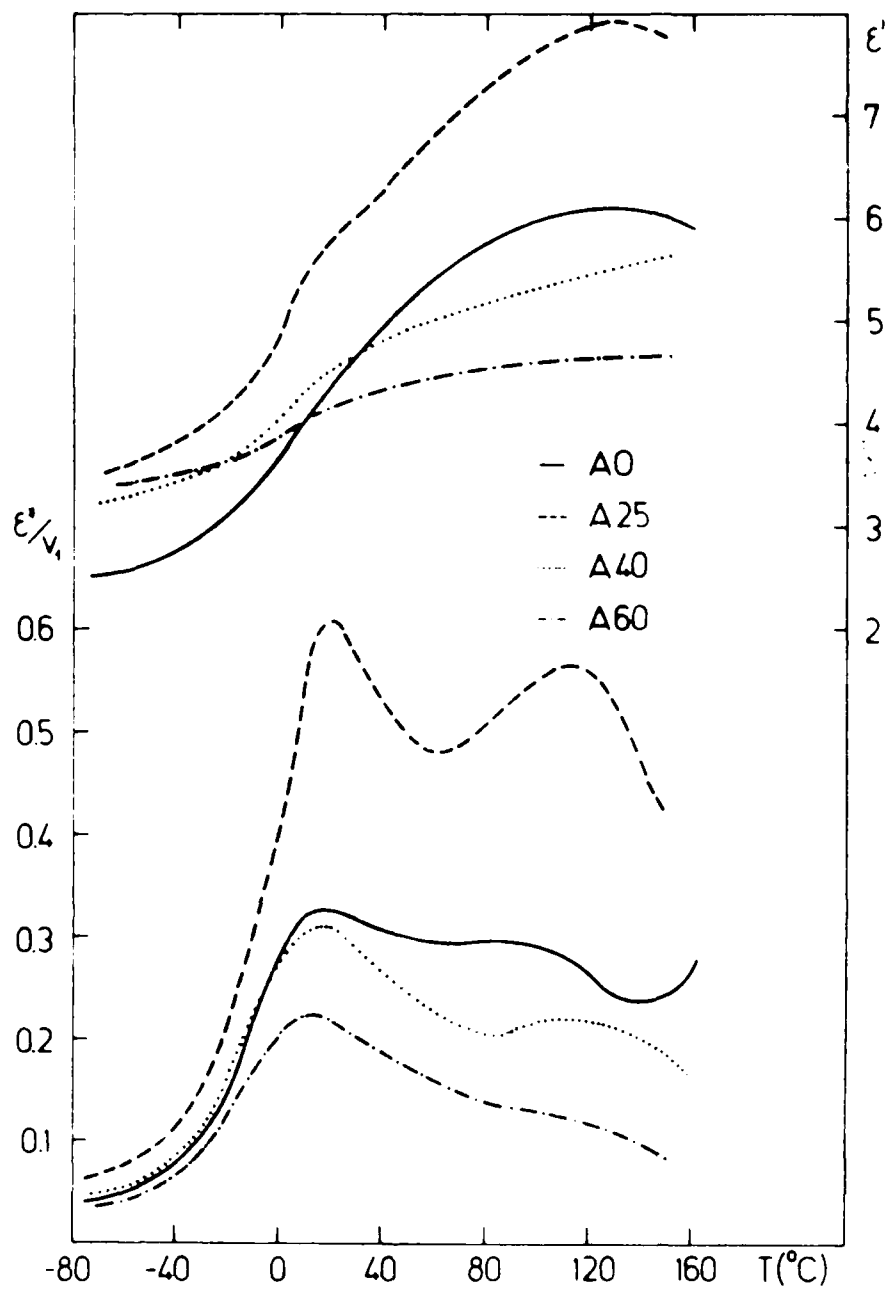
| ϵ_1 | ϵ_2 | σ_1 | σ_2 | $\bar{\epsilon}_\infty$ | $\bar{\epsilon}_s$ | τ (s) | ν_{\max} (Hz) |
|--------------|--------------|---------------------|---------------------|-------------------------|--------------------|----------------------|-------------------|
| 2.5 | 8.0 | 2×10^{-12} | 2×10^{-11} | 4.03 | 4.85 | 5.7×10^{-2} | 2.8 |
| 2.5 | 8.0 | 2×10^{-11} | 2×10^{-11} | 4.03 | 4.70 | 1.6×10^{-2} | 10 |
| 5.0 | 8.0 | 4×10^{-11} | 2×10^{-10} | 6.07 | 7.35 | 6.9×10^{-3} | 23 |
| 5.0 | 8.0 | 4×10^{-10} | 2×10^{-10} | 6.07 | 6.60 | 1.4×10^{-3} | 120 |
| 7.0 | 8.0 | 2×10^{-10} | 5×10^{-10} | 7.39 | 7.98 | 2.5×10^{-3} | 65 |
| 7.0 | 8.0 | 2×10^{-9} | 5×10^{-10} | 7.39 | 7.99 | 3.7×10^{-4} | 420 |

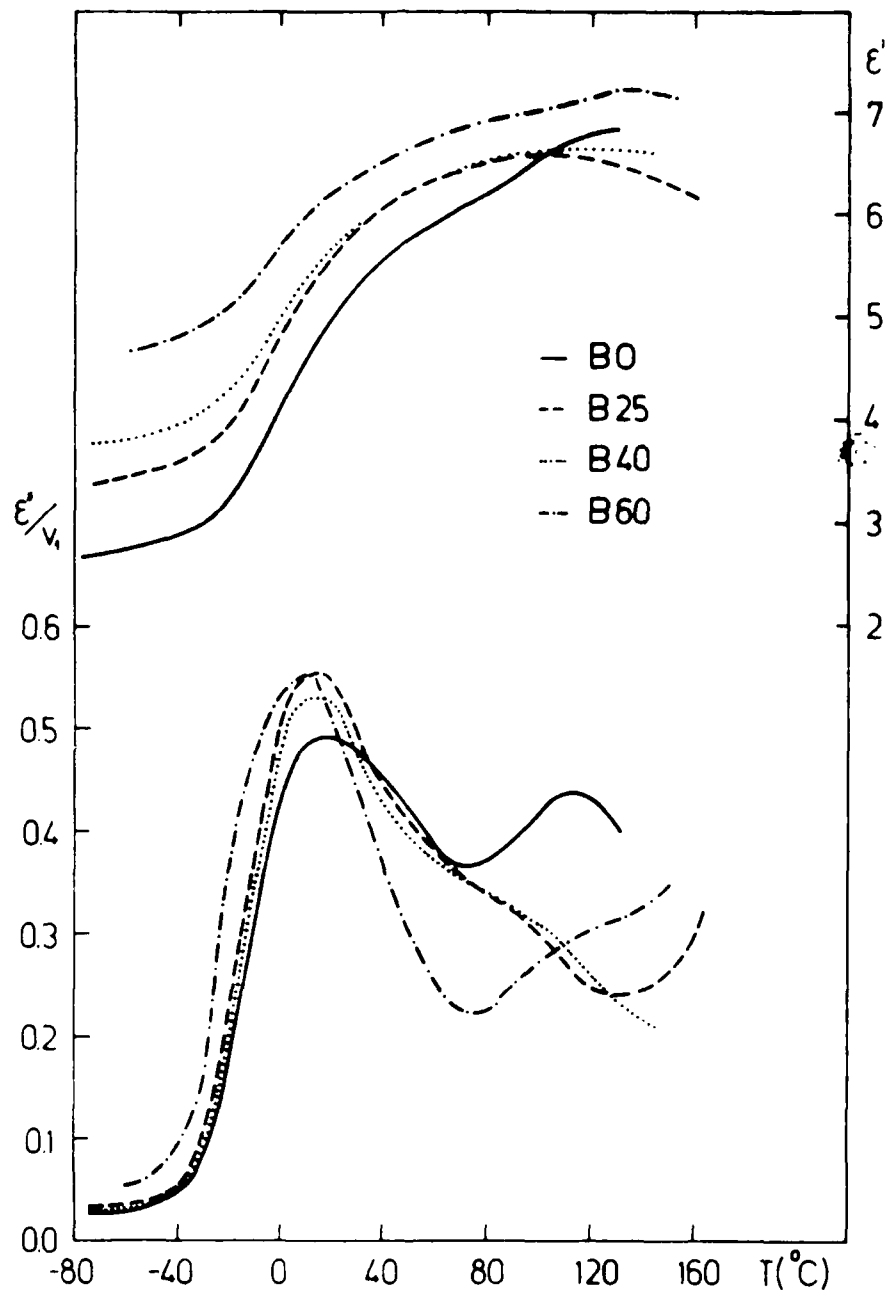
Figure Captions

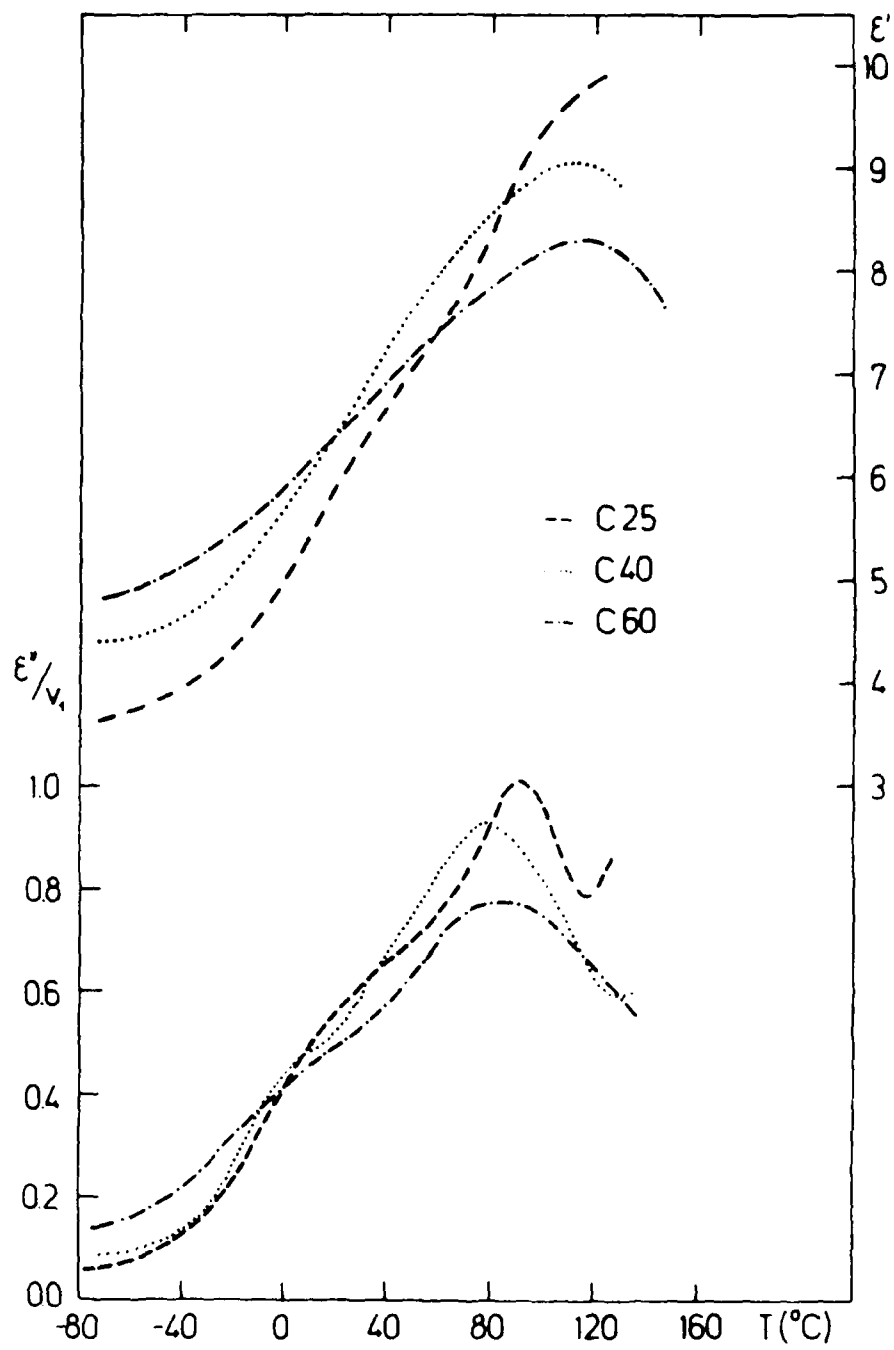
- Figure 1: Chemical structures of the polymer investigated.
- Figure 2: Dielectric dispersion and loss of the pure polymeric components at 100 kHz.
- Figure 3: Dielectric dispersion and loss of the A0 sample at four different frequencies.
- Figure 4: Dielectric dispersion and normalized loss of series A samples at 100 kHz.
- Figure 5: Dielectric dispersion and normalized loss of series B samples at 100 kHz.
- Figure 6: Dielectric dispersion and normalized loss of series C samples at 100 kHz.
- Figure 7: Permittivity differences as a function of temperature for series A.
- Figure 8: Permittivity differences as a function of temperature for series B.
- Figure 9: Permittivity differences as a function of temperature for series C.
- Figure 10: Arrhenius plots of the soft segment transition frequencies for A and B series.
- Figure 11: Arrhenius plot of 300 Hz AC conductivities of A, B and C series.
- Figure 12: Composite permittivities as a function of matrix permittivity calculated using $\epsilon_2 = 8.0$ and eq. (5).
- Figure 13: Ratio of loss maxima of the composite and the unfilled polymer calculated using eqs. (5) and (6). v_2 and ϵ_1 as indicated.











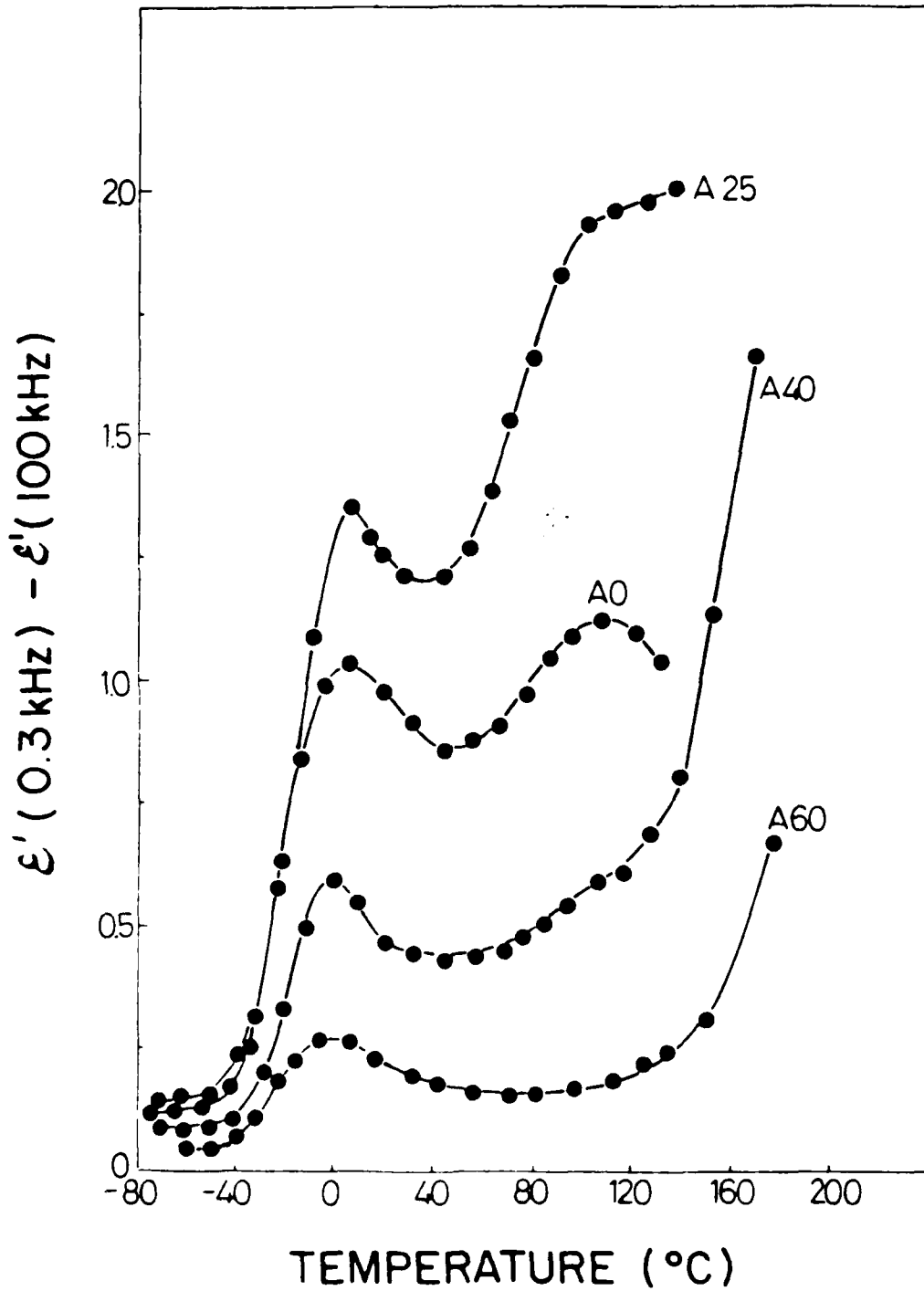


Fig. 1. $\epsilon' (0.3 \text{ kHz}) - \epsilon' (100 \text{ kHz})$

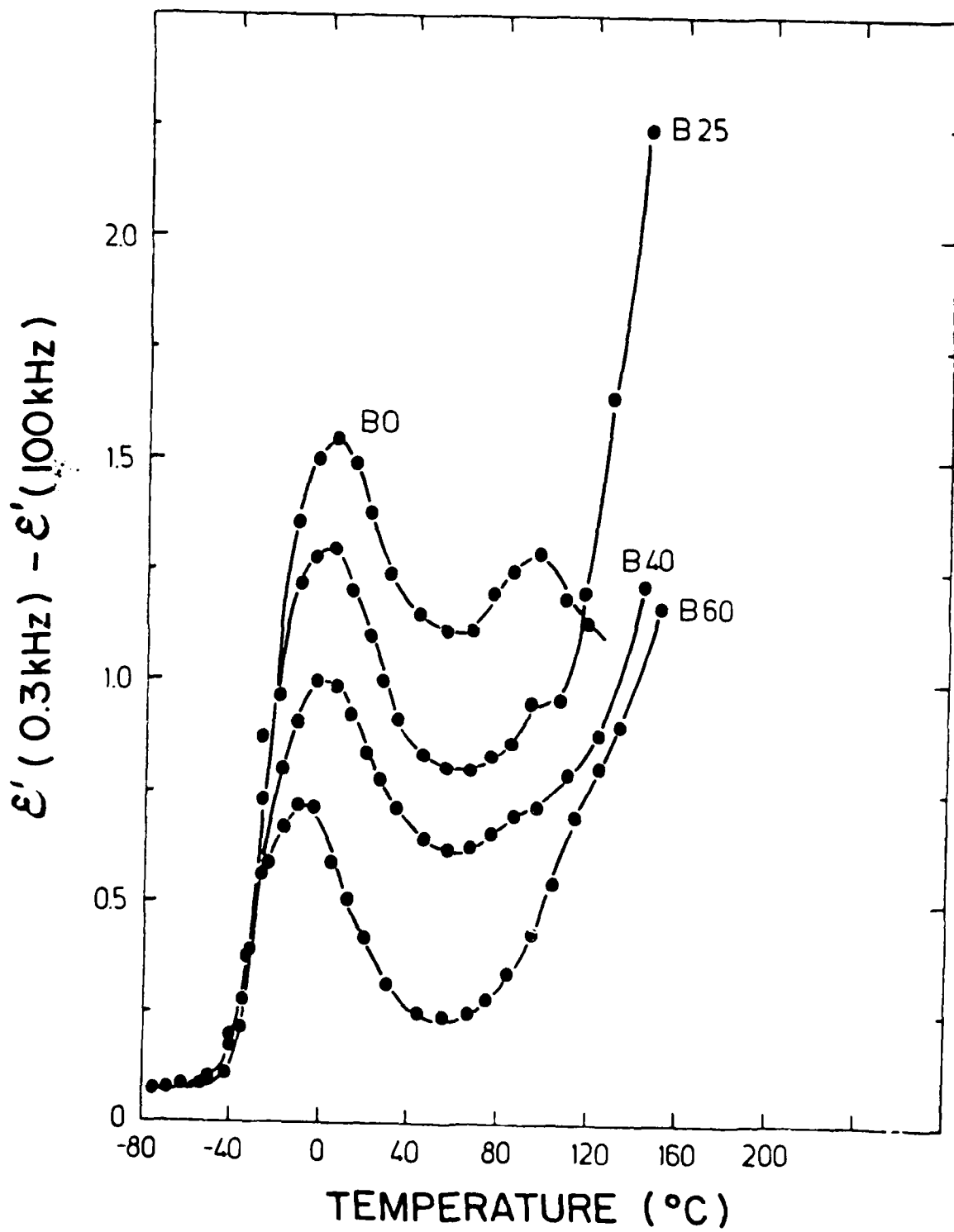
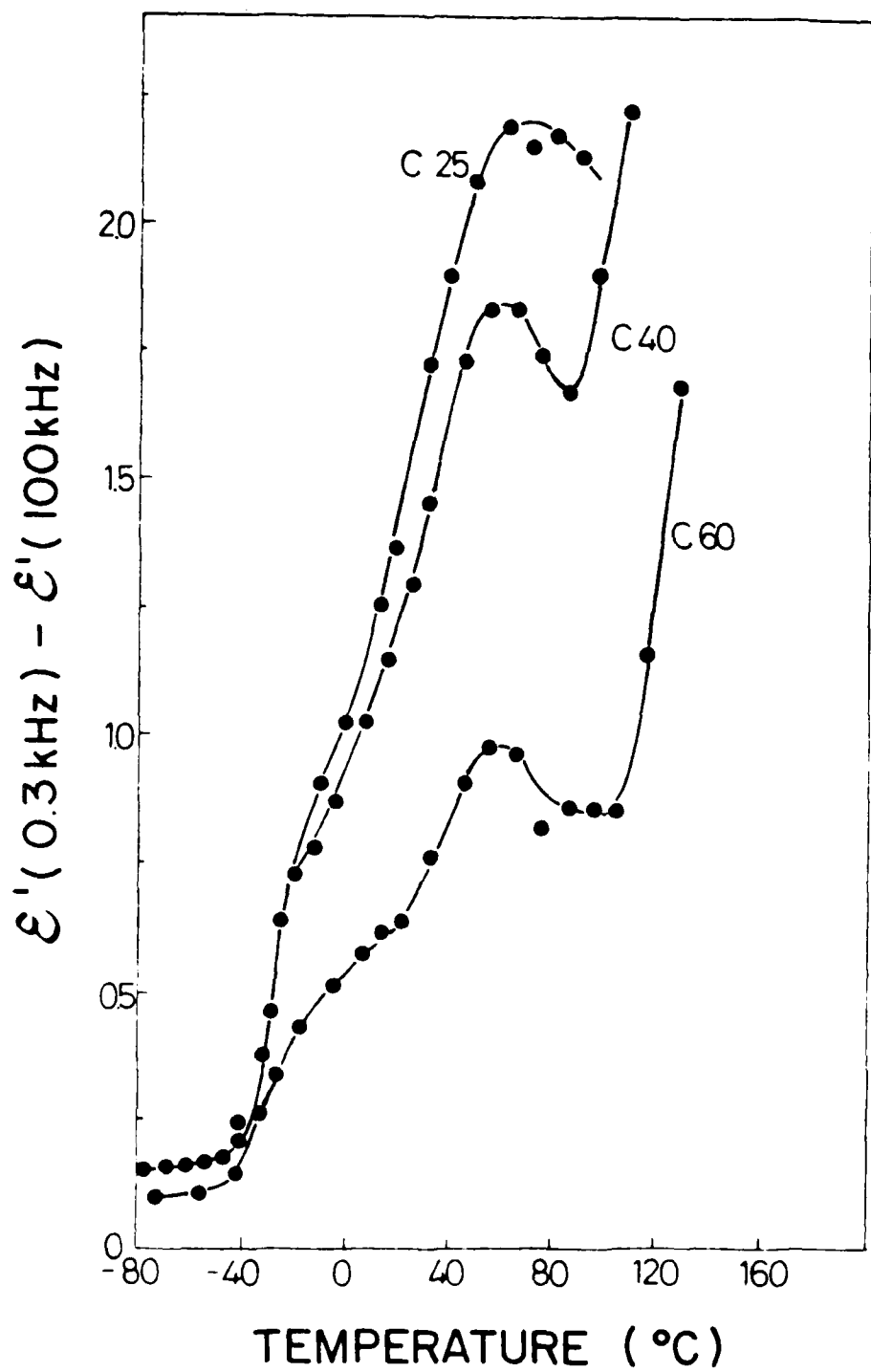


Fig. 2. Dielectric loss



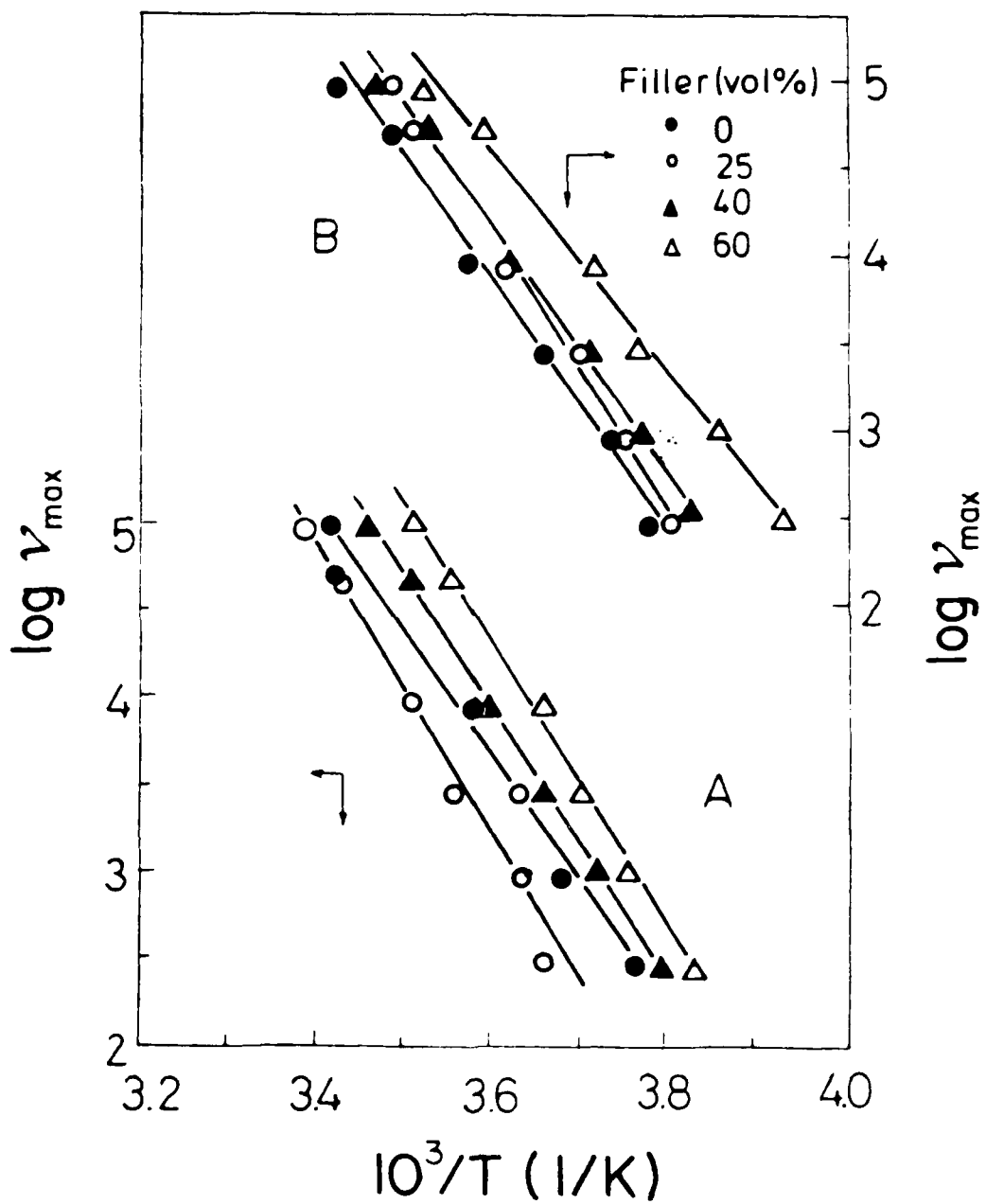
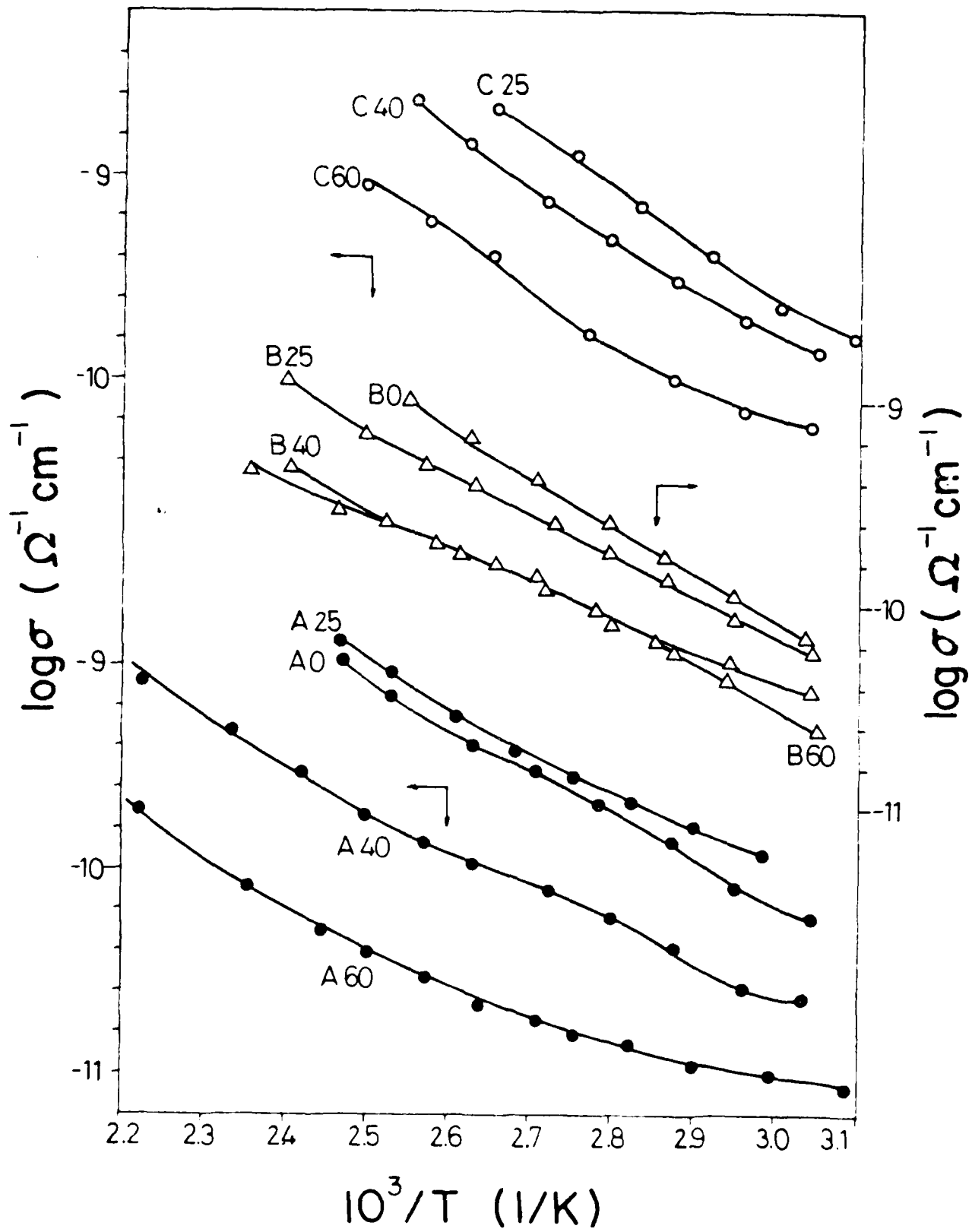
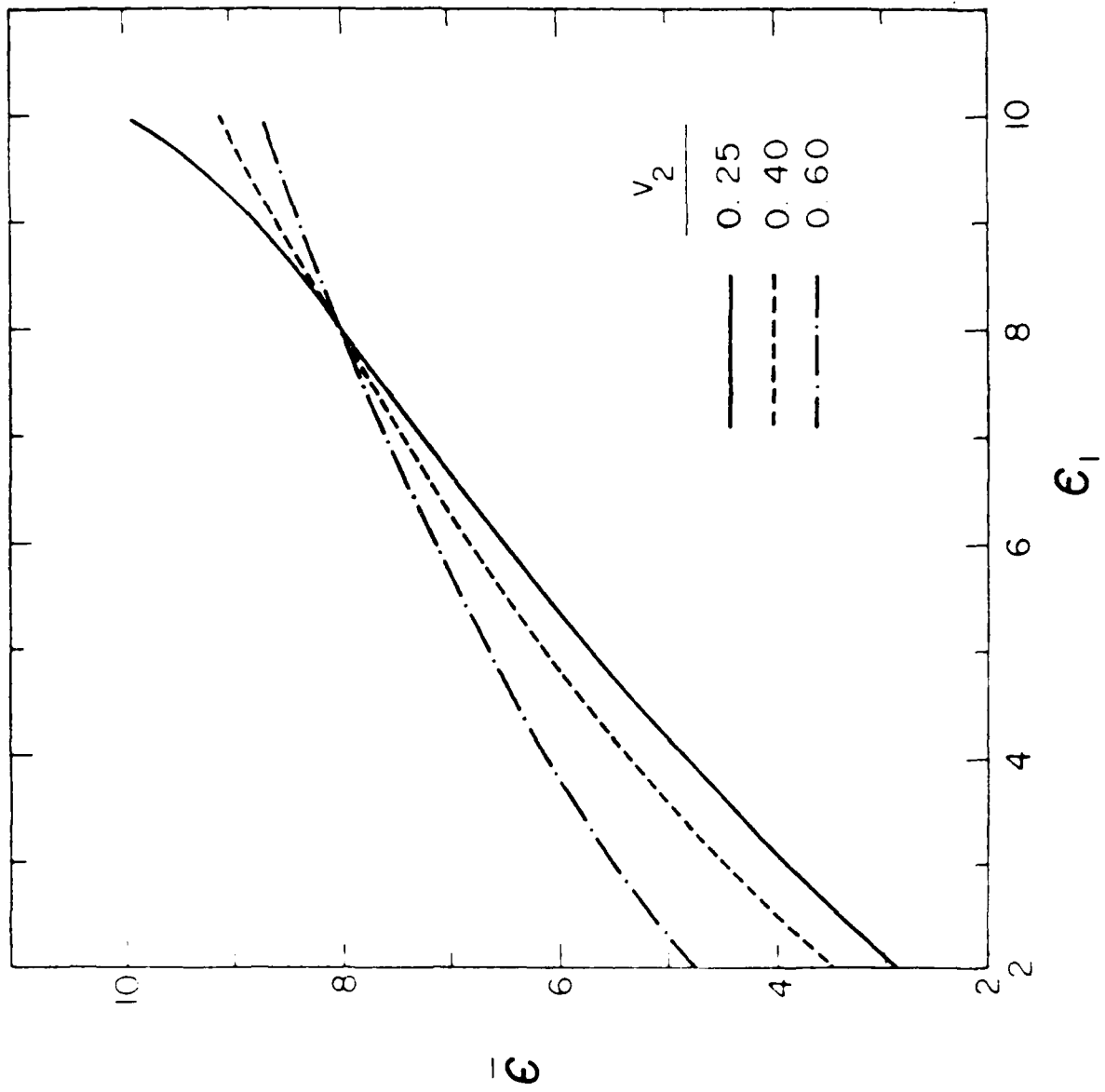


Fig. 10 *Frequency*
dependence





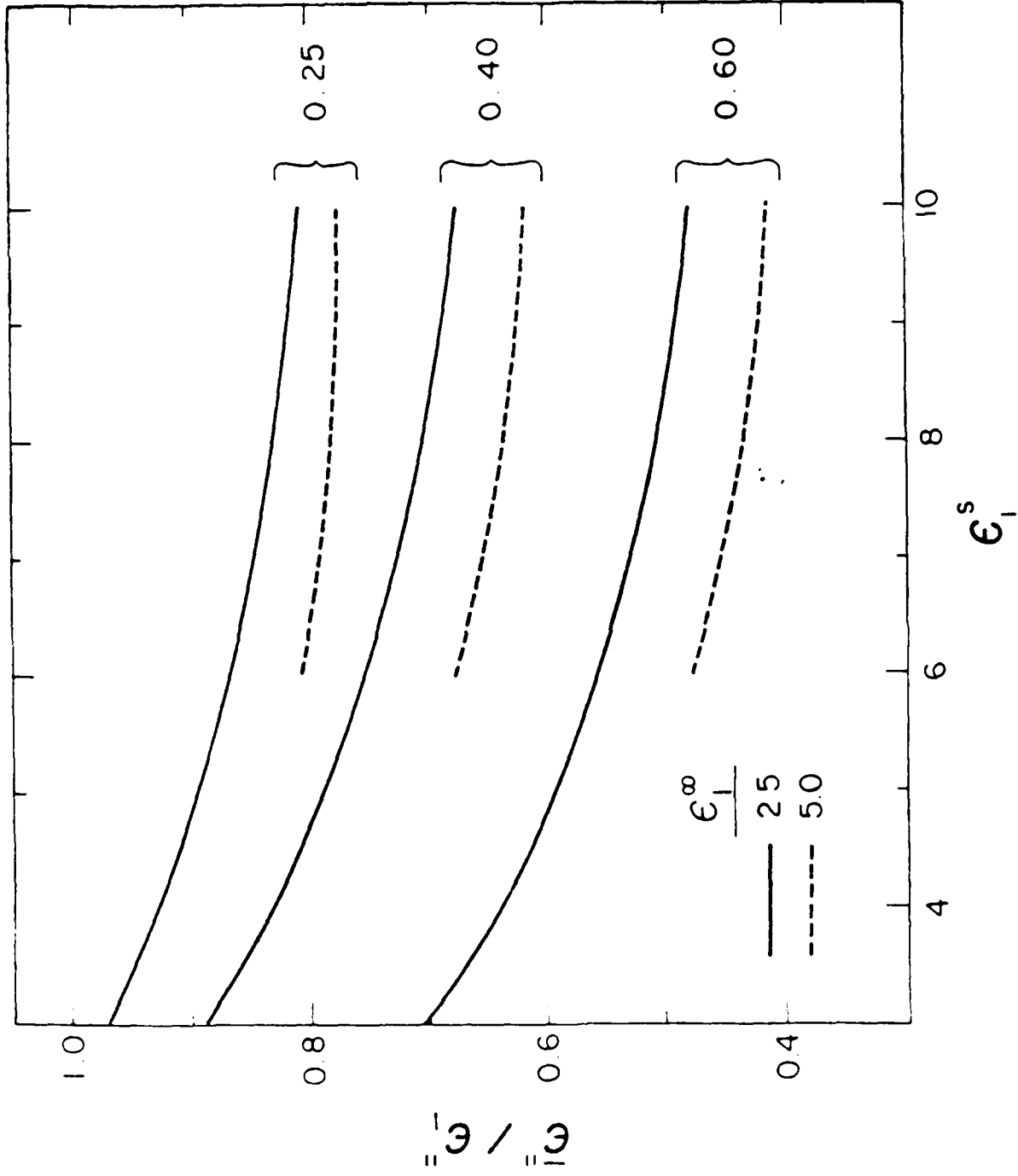


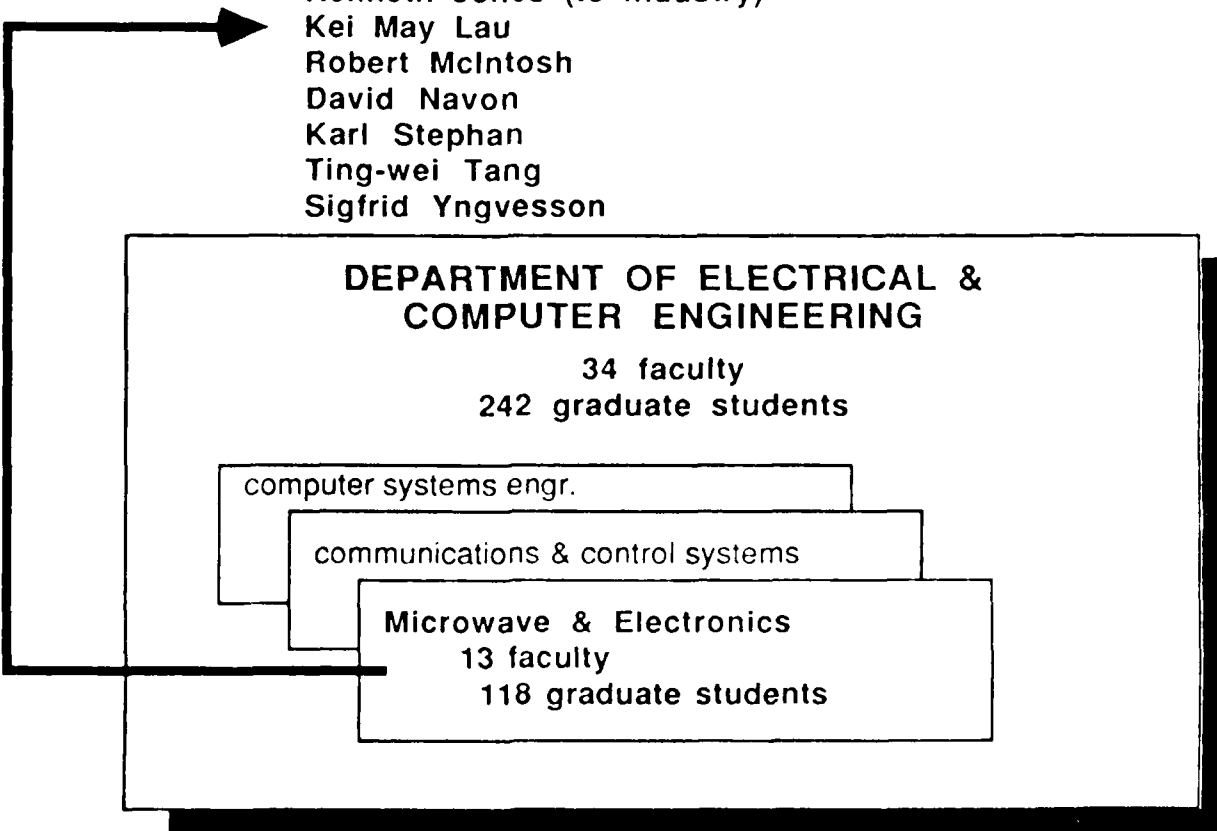
FIG. 10. VARIATION OF $\frac{V_1}{V_2}$ WITH P_1^s

MATERIALS RESEARCH
LABORATORY IN
POLYMERS

POLYMERS IN ELECTRONICS

- GaAs MESFETs with a polyimide passivant
- Microwave properties of polymers

Professors Robert Jackson
Kenneth Jones (to industry)
Kei May Lau
Robert McIntosh
David Navon
Karl Stephan
Ting-wei Tang
Sigfrid Yngvesson



DEPARTMENT OF ELECTRICAL & COMPUTER ENGINEERING

*MICROWAVE ELECTRONICS PROGRAM
PRESENT & FUTURE*

CURRENT MICROWAVE ELECTRONICS PROGRAM THRUSTS

13 faculty 118 graduate students

- Compound semiconductor materials & devices (III-V)
- Optoelectronics & very high speed integrated devices
- Numerical modeling of semiconductors
- Monolithic millimeter-wave materials & devices
- Antennas & radiating structures
- Microwave/millimeter systems
- Electromagnetics
- Microwave remote sensing

PLANS FOR NEXT TWO YEARS

- Hire 2-3 faculty in solid state electronics area
- Expand III-V materials, device and optoelectronics research
- Interdisciplinary research on GaAs/polymers & polymer properties

END

DTIC

7-86